2012 22nd International Lightning Detection Conference
2 – 3 April • Broomfield, Colorado, USA
4th International Lightning Meteorology Conference
4 – 5 April • Broomfield, Colorado, USA

LIGHTNING ACTIVITY IN A HAIL-PRODUCING STORM OBSERVED WITH PHASED-ARRAY RADAR

Donald R. MacGorman[1,2], Christopher Emersic[2], Pamela L. Heinselman[1]
[1]NOAA/National Severe Storms Laboratory, Norman, Oklahoma, USA
[2]Cooperative Institute for Mesoscale Meteorological Studies, University of Oklahoma and NOAA/National Severe Storms Laboratory, Norman, Oklahoma, USA

1. Introduction

This study examines lightning activity relative to the rapidly evolving kinematics of a hail-producing multicell storm on 15 August 2006. Data were provided by the National Weather Radar Testbed Phased-Array Radar (NWTPR), the Oklahoma Lightning Mapping Array (OK-LMA), and the United States National Lightning Detection Network (US-NLDN). The S-Band phased-array radar provided reflectivity and radial velocity structure at a temporal resolution of <1 min.

2. Relationships with Flash Rates

This study begins with a period of storm intensification following several less intense cells (Figs. 1–3). We observed two 6–10 min periods of rapid substantial increases in flash rates. Both would satisfy some definitions for “lightning jumps,” which have been suggested as flags of storm intensification leading to increased probability of severe weather (e.g. Williams et al. 1999; Schultz et al. 2009). The flash rate increases coincided with two updraft pulses inferred from reflectivity and radial velocity observations, a relationship that is in full agreement with the findings of several studies (MacGorman et al. 1989; Ziegler and MacGorman 1994; Williams et al. 1999; Krehbiel et al. 2000; Goodman et al. 2005; Wiens et al. 2005).

The first and smaller of the two analyzed updraft pulse began at approximately 2220 UTC (Figs. 1 and 2). As the height and horizontal extent of the 40 dBZ reflectivity increased indicating the updraft pulse was intensifying, total flash rates in the storm increased to ~220 min^{-1}. This updraft pulse was not related to severe weather production at all, although it was related to storm growth. Flash rates leveled off during the cell’s first mature stage, after precipitation in the cell reached the ground at approximately 2225 UTC and the 40 dBZ contour reached its maximum height at approximately 2226 UTC.

At approximately 2226 UTC, the first evidence of a second updraft pulse appeared in reflectivity (Fig. 1) and radial velocity structure (not shown). By 2228, the formation of the second pulse was clear in the arced horizontal extension of 40 dBZ reflectivity between 4 and 8 km MSL. At 2228:54 UTC, a three-body scatter spike (TBSS) began to develop at approximately 7 km MSL in the second updraft pusle, as the reflectivity tower from the first pulse started weakening. Zrnic (1987) found that the TBSS, in combination with the very large reflectivities (> 65 dBZ) in the mixed phase region, is indicative of large, wet hail. At 2231 UTC – 2234 UTC, as the range and depth of the TBSS and the width and depth of reflectivities > 65 dBZ both increased in the mixed phase region of the second updraft pulse, total flash rates in the storm decreased. It is unusual for flash rates to decrease as the horizontal and vertical extent of moderate to large reflectivities increase in the mixed phase region.

We suggest that this reduction in flash rate was likely related to hail in some regions being in a state of surface wet growth. Wet growth is not conducive to hydrometeor charging because it tends to reduce rebounding from graupel-ice collisions, and so reduces the amount of charge separated by rebounding collisions. Support for this interpretation is provided by the formation of a “lightning hole” or a “lightning ring,” which consists of larger VHF source densities surrounding a pronounced minimum a few kilometers in diameter (Fig. 4). Several observational and simulation studies have found that lightning channels develop more densely in regions with larger charge density and tend to avoid regions with little or no net charge (MacGorman et al. 1981, 1983, 2001; Williams 1985; Mansell et al. 2002; Coleman et al. 2003), so the pronounced minimum in lightning density probably indicates a significantly smaller charge density there. As in previous studies (e.g., Krehbiel et al. 2000; MacGorman et al. 2005, 2008; Payne et al. 2010), the lightning hole is associated with an updraft, but unlike all previous studies, the lightning hole on 15 August 2008 did not involve a rotating updraft (i.e., a mesocyclone) and a bounded weak echo region, but rather involved an updraft containing large reflectivities and hail in wet growth.

The height and width of the 40 dBZ reflectivity continued to increase through 2241 UTC, eventually reaching an altitude of approximately 13 km MSL (Fig. 5). As the height of the storm increased, both the largest reflectivities and the TBSS descended and weakened, indicating that wet hail was descending below the mixed phase region. During this period, total flash rates again began increasing, eventually reaching ~450 min^{-1} (Fig. 3), probably due to the increasing storm volume and the inferred graupel volume and the decreasing region involved in wet hail growth. The volume of reflectivity >40 dBZ above the -20 ℃ isotherm reached its peak at approximately 2240 - 2242 UTC. Shortly afterward the updraft pulse began weakening as the larger reflectivities above the -20 ℃ isotherm began decreasing and its height began descending (see 224156 – 224405 in Fig. 5). Flash rates began their steady decrease as the storm weakened, eventually dissipating (Fig. 3).

3. Cloud-to-Ground Flash Polarity and Flash Rate

Only 37 ground flashes were reported by the NLDN in the storm analyzed here, and only six were confidently verified as ground flashes by comparison with associated LMA data. Of the six likely ground flashes, the first two occurred during the first updraft pulse mentioned above (period 1) and lowered the usual negative charge to ground (negative ground flashes), with low peak currents of -7.8 and -9.2 kA (Fig. 2). All four of the ground flashes that lowered positive charge (positive ground flashes, with peak currents of +15.3, +133.9, +107.4, and +66.6 kA, respectively) occurred during the second, stronger updraft pulse (period 2), when the total flash rate grew to be much greater than the maximum observed during period 1 (Fig. 3). The first positive ground flash occurred ~5 min before the main hail region was inferred from radar data to have reached ground, with the rest occurring later, behavior similar to that observed by MacGorman and Burgess (1994). No further ground flashes were detected during the rest of the storm's lifetime.

Negative ground flashes were initiated between a midlevel region of negative charge and a lower region of positive charge that existed during the first updraft surge. The source of the lower positive charge thought to be necessary for producing most negative ground flashes (e.g. Jacobson and Krider 1976; MacGorman et al. 2001; Mansell et al. 2002) has been a matter of some debate. Laboratory experiments indicate that graupel tends to charge positively at higher temperatures (e.g. Takahashi 1978; Saunders and Peck 1998; Saunders et al. 2004; Emersic and Saunders 2010). The lower positive charge region observed in this storm was most likely caused by graupel that had interacted with ice crystals in environments warmer than roughly -10°C). The development of the upper region of positive charge involved in cloud flashes in the region of the first updraft pulse we analyzed occurred later in the period, after the lower two charge regions had already formed, and is consistent with many studies and observations suggesting that lighter ice crystals rising in the updraft were the charge carriers for the uppermost positive charge.

Positive ground flashes occurred as the storm intensified and were initiated between a new deep midlevel region of positive charge and a transient lower region of negative charge through which lightning leaders propagated to ground. The positive charge through which positive ground flashes propagated formed in the updraft surge during period 2 and had no low-level negative charge directly below it. Several studies (e.g. Wiens et al. 2005; Williams et al. 2005; Carey and Buffalo 2007) have suggested that strong broad updrafts are more conducive to the formation of midlevel positive charge, because laboratory studies (e.g. Saunders et al. 2004; Saunders et al. 2006; Emersic and Saunders 2010) have found that graupel tends to gain positive charge when interacting with rising small cloud ice particles (which would gain negative charge) in regions of relatively large liquid water content, across a broad range of environmental temperature. MacGorman et al. (2008) noted that this process would produce a negative dipole charge structure, with negative charge only above the positive charge. From cloud flash morphology, we inferred that the upper region of this part of the storm contained negative charge, consistent with what would be expected from graupel-ice interactions in regions of large liquid water content.

The lower negative charge thought to be necessary to initiate most positive ground flashes (e.g. MacGorman et al. 2001; Mansell et al. 2002) appeared in this case to be the descending remnant of the previous midlevel negative charge as the region of the first updraft pulse produced a downdraft. The overall charge structure of the two adjoining regions consisted of a descending normal polarity structure (midlevel negative charge, with positive charge above and below it, formed during period 1) next to a new inverted polarity structure (upper negative charge above midlevel positive charge, formed during period 2). Thus, positive ground flashes occurred because the midlevel positive charge in the newer region interacted with a negative charge (previously formed at midlevels) that had fallen to lower altitudes, as hypothesized by MacGorman et al. (2008). The complex temporal and spatial evolution of the charge regions throughout the storm's lifetime is consistent with suggestions that the charge structure of a storm is not a product just of the charge generated locally, but also is a result of the history and transport of charge carriers in the cloud, as noted by MacGorman et al. (2008) and Bruning et al. (2010).

Many thousands of flashes occurred in this storm, but less than 1% of the flashes were cloud-to-ground flashes. Several other studies (e.g. Rust et al. 1981; MacGorman et al. 1989; Carey and Rutledge 1998; Shafer et al. 2000) have similarly noted that cloud-to-ground flashes compose only a small percentage of all flashes in many severe storms, particularly in storms whose vertical polarity of charge structure is opposite to the usual polarity (i.e., negative charge is uppermost in the main tripole or dipole involved in lightning, instead of the usual positive charge) or which produce ground flashes lowering positive charge to ground, instead of the usual negative charge.

MacGorman et al. (1989; 2005; 2007) suggested in other cases that the small fraction of flashes striking ground was caused by a severe storm's very strong updraft. The strong updraft lifted the formation and growth of the frozen hydrometeor charge carriers to higher altitudes than usual in storms, and caused the resulting charge to remain relatively high for substantial periods. Because cloud-to-ground flashes require not only a degree of electrification strong enough to initiate flashes, but a configuration of cloud charge that would cause a channel to propagate to ground, they argued that the higher altitude and close proximity of oppositely charged regions resulting from strong updrafts in severe storms were more favorable than usual for cloud flashes and less favorable than usual for the formation of a cloud-to-ground channel. MacGorman et al. (1989; 2005; 2007) also noted that cloud-to-ground lightning production may be inhibited in severe storms by the time required to form and transport downward the precipitation carrying the low-level charge region, which is needed to initiate lightning from the oppositely charged midlevel charge region. These arguments are consistent with our findings of substantial cloud lightning during a time when an elevated and horizontal dipole charge structure was present, and with the increased lightning ground flash occurrence when transient lower charge regions were present as discussed above.

4. High-altitude Bands of VHF Radiation

One aspect of our study for which high-temporal resolution NWRT PAR data were important was an analysis of a transient, upper band of VHF radiation consisting of a fairly steady rate of mostly single isolated VHF sources, which occurred during two episodes (approximately 2226 – 2230 UTC and 2235 – 2243 UTC in Fig. 2). The initial occurrence of this band coincided with the initial strong, vertical growth during period 1. The first upper band of isolated VHF radiation sources began when the region of 40-dBZ reflectivity reached a maximum altitude of approximately 10 km, and it ceased as the maximum height of 40-dBZ reflectivity began decreasing in the storm 3–4 min later. (There was no upper band of VHF radiation for previous storms, which were shallower.) This VHF radiation occurred at an altitude of ~13–15 km, above a vertically growing reflectivity echo, and was 1–4 km above the highest region of 30-dBZ reflectivity for the entire period of its occurrence. It appears that the reflectivity at the location of most upper sources was below the minimum detectable level of the NWRT PAR, but it is possible that radar side-lobe contamination obscured some features near storm top in the vicinity of the upper VHF sources for at least part of the period.

The second transient upper band of isolated VHF sources began approximately 6 min later, when the 40-dBZ reflectivity echo of the second updraft surge reached its maximum altitude of approximately 13 km in period 2, and again ended when the larger reflectivities began decreasing in the upper part of the storm 4 min later. Like the first band, these VHF sources were at an altitude of approximately 15 km, but unlike the first band, 30-dBZ reflectivity extended up almost to 15 km throughout the period in which the band occurred. Also unlike the first band, which appeared abruptly at 15 km, the second band appeared to be the apex of a rising relative maximum of lightning density (a feature Ushio et al. (2003) called a “lightning bubble”) which had begun rising 2 min earlier from an altitude of approximately 11 km (Fig. 2). There was also a coincident increase in the maximum height of larger reflectivities. The high temporal resolution of NWRT PAR allowed us to directly observe this relationship between the high isolated VHF sources and the increasing altitude of the storm.

It is not clear from our data what caused this upper band of continual single radiation sources. The lower threshold for electric field breakdown at upper altitudes of the storm probably was a factor. Taylor et al. (1984), who observed somewhat similar continual, scattered VHF sources in the upper part of a severe storm, suggested that the discharges occurred between the uppermost charge inside the thunderstorm and screening layer charge that formed on the cloud boundary (e.g., section 3.5.4, MacGorman and Rust 1998). Regarding our observation of lightning in the overshooting top, it is possible that eddies along the cloud boundary may have folded screening layer charge into the cloud interior to interact with charge rising in the updraft and thereby to produce electric field magnitudes large enough to cause lightning. Such a possibility is supported by the observations of Blythe et al. (1988) and Stith (1992), who used tracers to show that the upper cloud boundary is entrained into the upper cloud. Polarimetric radar data or in-situ measurements may be needed to shed more light on this phenomenon.

5. Closing Comments

The frequent volume scans provided by the NWRT PAR demonstrated here that using a peak in flash rates to identify the time of a relative maximum in storm intensity can be misleading in some circumstances. It is true that the initial rapid increase in flash rates was indicative of storm intensification, but flash rates subsequently increased more slowly and then decreased as the storm’s first downdraft developed and an updraft surge began simultaneously. The offsetting growth and decay within the storm probably contributed to the timing of the peak in flash rates. Another factor was the initial appearance and growth of a region in which a TBSS and reflectivity >60 dBZ indicated the growth of wet hail beginning in the second updraft surge. As discussed previously, graupel wet growth would not be expected to contribute to electrification by charge exchange during collisions with cloud ice, because the cloud ice rarely, if ever, rebounds under such conditions. Thus, a significant portion of mixed-phase precipitation growth probably did not contribute to the storm’s electrification during the period of wet hail growth, and this likely contributed to the 2-min decrease in flash rates which followed the initial peak and preceded the second, more rapid increase in flash rates.

The above relationships suggest that lightning data provide additional information about storm intensification that could be useful to forecasters, with two cautions:

1. As an indication of sudden changes in the updraft mass flux through the mixed-phase region, rapidly increasing flash rates can be broadly useful in nowcasting increased potential for severe weather in the 0–20 min time frame, but in much the same way as hook echoes and mesocyclones are not direct indicators of tornadoes, lightning jumps should not be confused as an indicator of a severe weather phenomenon itself (Williams 2001). Schultz et al. (2009) show that a suitable algorithm for detecting lightning jumps can show positive correlation with severe weather reports under at least some scenarios, even though the electrical measurements do not directly detect the severe phenomena of interest.
2. One must be somewhat cautious when interpreting peaks in flash rates. Although each tall updraft

pulse in a storm contributes additional electrification, the timing of major inflections, peaks, or minima in lightning flash rates of the storm overall can depend on the competing tendencies from co-evolving updraft and downdraft developments in different regions of the storm. Furthermore, one exception to the tendency for increasing electrification during precipitation growth in the mixed phase region appears to be the situation in which the surface of frozen precipitation becomes wet. Thus, while a large rapid increase in lightning flash rates reliably indicates the growth of a storm through and above the mixed phase region, level or decreasing storm flash rates do not necessarily imply that updrafts or storms are in steady state or weakening.

6. Acknowledgments

Funding for this research was provided by NSF grant ATM-0813767 and ATM-0233268. Funding also was provided by NOAA/Office of Oceanic and Atmospheric Research under NOAA - University of Oklahoma Cooperative Agreement #NA11OAR4320072, U.S. Department of Commerce. Any opinions, findings, conclusions, or recommendations expressed in this paper are those of the authors and do not necessarily reflect the views of the National Science Foundation. The authors thank Drs. Ron Thomas, Bill Rison, Paul Krehbiel, and Eric Bruning for their help with data analysis, support with the required software and hardware, and assistance in general.

7. References

Blythe, A. M., W. A. Cooper, and J. B. Jensen, 1988: A study of the source of entrained air in Montana cumuli. *J. Atmos. Sci.*, **45,** 3944–3964.

Bruning, E. C., W. D. Rust, T. J. Schuur, D. R. MacGorman, P. R. Krehbiel, and W. Rison, 2007: Electrical and Polarimetric Radar Observations of a Multicell Storm in TELEX. *Mon. Wea. Rev.*, **135,** 2525–2544, doi:10.1175/MWR3421.1.

Bruning, E. C., W. D. Rust, D. R. MacGorman, M. I. Biggerstaff, and T. J. Schuur, 2010: Formation of charge structures in a supercell. *Mon. Wea. Rev.***,** in press, doi:10.1175/2010MWR3160.1.

Carey, L. D., and S. A. Rutledge, 1998: Electrical and multiparameter radar observations of a severe hailstorm. *J. Geophys. Res.*, **103,** 13979–14000.

Carey, L. D., and K. M. Buffalo, 2007: Environmental control of cloud-to-ground lightning polarity in severe storms. *Mon. Wea. Rev.*, **135,** 1327–1353.

Coleman, L. M., T. C. Marshall, M. Stolzenburg, T. Hamlin, P. R. Krehbiel, W. Rison, and R. J. Thomas, 2003: Effects of charge and electrostatic potential on lightning propagation. *J. Geophys. Res.*, **108,** 4298, doi:10.1029/2002JD002718.

Emersic, C., and C. P. R. Saunders, 2010: Further laboratory investigations into the Relative Diffusional Growth Rate theory of thunderstorm electrification. *Atmos. Res.*, doi:10.1016/j.atmosres.2010.07.011.

Emersic, C., P. L. Heinselman, D. R. MacGorman, and E. Bruning, 2011: Lightning activity in a hail-producing storm observed with phased-array radar. *Mon. Wea. Rev.*, **139**, 1809-1825, doi: 10.1175/2010MWR3574.1.

Goodman, S. J., R. Blakeslee, H. Christian, W. Koshak, J. Bailey, J. Hall, E. McCaul, D. Buechler, C. Darden, J. Burks, T. Bradshaw, and P. Gatlin, 2005: The North Alabama Lightning Mapping Array: Recent severe storm observations and future prospects. *Atmos. Res.*, **76,** 423–437.

Jacobson, E. A., and E. P. Krider, 1976: Electrostatic field changes produced by Florida lightning. *J. Atmos. Sci.*, **33,** 103–117.

Krehbiel, P. R., R. J. Thomas, W. Rison, T. Hamlin, J. Harlin, and M. Davis, 2000: GPS-based mapping system reveals lightning inside storms. *EOS, Trans. Amer. Geophys. Union*, **81,** 21–25.

MacGorman, D. R., A. A. Few, and T. L. Teer, 1981: Layered lighting activity. *J. Geophys. Res.*, **86,** 9900–9910.

MacGorman, D. R., W. L. Taylor, and A. A. Few, 1983: Lightning location from acoustic and VHF techniques relative to storm structure from 10 cm radar. *Proc. Atmos. Elec.*, eds. L. H. Ruhnke and J. Latham, A. Deepak Publishing, Hampton, VA, 377–380.

MacGorman, D. R., D. W. Burgess, V. Mazur, W. D. Rust, W. L. Taylor, and B. C. Johnson, 1989: Lightning rates relative to tornadic storm evolution on 22 May 1981. *J. Atmos. Sci.*, **46,** 221–250.

MacGorman, D. R., and D. W. Burgess, 1994: Positive cloud-to-ground lightning in tornadic storms and hailstorms. *Mon. Wea. Rev.*, **122,** 1671–1697.

MacGorman, D. R., and W. D. Rust, 1998: *The Electrical Nature of Storms*. Oxford University Press, 442 pp.

MacGorman, D. R., J. M. Straka, and C. L. Ziegler, 2001: A lightning parameterization for numerical cloud models. *J. Appl. Meteor.*, **40,** 459–478.

MacGorman, D. R., W. D. Rust, P. Krehbiel, W. Rison, E. Bruning, and K. Wiens, 2005: The electrical structure of two supercell storms during STEPS. *Mon. Wea. Rev.*, **133,** 2583–2607.

MacGorman, D. R., T. Filiaggi, R. L. Holle, and R. A. Brown, 2007: Negative cloud-to-ground lightning flash rates relative to VIL, maximum reflectivity, cell height, and cell isolation. *J. Lightning Res.*, **1,** 132–147.

MacGorman, D. R., W. D. Rust, T. J. Schuur, M. I. Biggerstaff, J. M. Straka, C. L. Ziegler, E. R. Mansell, E. C. Bruning, K. M. Kuhlman, N. R. Lund, N. S. Biermann, C. Payne, L. D. Carey, P. R. Krehbiel, W. Rison, K. B. Eack, and W. H. Beasley, 2008: TELEX: The Thunderstorm Electrification and Lightning Experiment. *Bull. Amer. Meteor. Soc.*, **89,** 997–1013, doi:10.1175/2007BAMS2352.1.

Mansell, E. R., D. R. MacGorman, J. M. Straka, and C. L. Ziegler, 2002: Simulated three-dimensional branched lightning in a numerical thunderstorm model. *J. Geophys. Res.*, **107,** 4075, doi:10.1029/2000JD000244.

Payne, C. D., T. J. Schuur, D. R. MacGorman, M. I. Biggerstaff, K. M. Kuhlman, and W. D. Rust, 2010: Polarimetric and electrical characteristics of a lightning ring in a supercell storm. *Mon. Wea. Rev.*, **138**, 2405–2425, doi: 10.1175/2009MWR3210.1.

Rust, W. D., W. L. Taylor, D. R. MacGorman, and R. T. Arnold, 1981: Research on electrical properties of severe thunderstorms in the Great Plains. *Bull. Amer. Meteor. Soc.*, **62,** 1286–1293.

Saunders, C. P. R., and S. L. Peck, 1998: Laboratory studies of the influence of the rime accretion rate on charge transfer during crystal/graupel collisions. *J. Geophys. Res.*, **103,** 13949–13956.

Saunders, C. P. R., H. Bax-Norman, E. E. Avila, and N. E. Castellano, 2004: A laboratory study of the influence of ice crystal growth conditions on subsequent charge transfer in thunderstorm electrification. *Quart. J. Roy. Meteor. Soc.*, **130,** 1395–1406.

Saunders, C. P. R., H. Bax-Norman, C. Emersic, E. E. Avila, and N. E. Castellano, 2006: Laboratory studies of the effect of cloud conditions on graupel/crystal charge transfer in thunderstorm electrification. *Quart. J. Roy. Meteor. Soc.*, **132,** 2653–2673.

Schultz, C. J., W. A. Petersen, and L. D. Carey, 2009: Preliminary development and evaluation of lightning jump algorithms for the real-time detection of severe weather. *J. Appl. Meteorol. Climatol.*, **48,** 2543–2563, doi:10.1175/2009JAMC2237.1.

Shafer, M. A., D. R. MacGorman, and F. H. Carr, 2000: Cloud-to-ground lightning throughout the lifetime of a severe storm system in Oklahoma. *Mon. Wea. Rev.*, **128,** 1798–1716.

Stith, J. L., 1992: Observations of cloud-top entrainment in cumuli. *J. Atmos. Sci.*, **49,** 1334–1347.

Takahashi, T., 1978: Riming electrification as a charge generation mechanism in thunderstorms. *J. Atmos. Sci.*, **35,** 1536–1548.

Taylor, W. L., E. A. Brandes, W. D. Rust, and D. R. MacGorman, 1984: Lightning activity and severe storm structure. *Geophys. Res. Lett.*, **11,** 545–548.

Ushio, T., S. J. Heckman, H. J. Christian, and Z. I. Kawasaki, 2003: Vertical development of lightning activity observed by the LDAR system: lightning bubbles. *J. Appl. Meteor.*, **42,** 165–174.

Wiens, K. C., S. A. Rutledge, and S. A. Tessendorf, 2005: The 29 June 2000 supercell observed during STEPS. Part II: Lightning and charge structure. *J. Atmos. Sci.*, **62,** 4151–4177.

Williams, E. R., 1985: Electrical discharge propagation in and around space charge clouds. *J. Geophys. Res.*, **90,** 6059–6070.

Williams, E. R., B. Boldi, A. Matlin, M. Weber, S. Hodanish, D. Sharp, S. Goodman, R. Raghavan, and D. Buechler, 1999: The behavior of total lightning activity in severe Florida thunderstorms. *Atmos. Res.*, **51,** 245–265.

Williams, E. R., 2001: The electrification of severe storms. In *Severe Convective* Storms, ed. C. A. Doswell, III, Amer. Meterolog. Soc. Monograph Series, **28** (50), p. 527–561.

Williams, E. R., V. Mushtak, D. Rosenfeld, S. Goodman, and D. Boccippio, 2005: Thermodynamic conditions favorable to superlative thunderstorm updraft, mixed phase microphysics and lightning flash rate. *Atmos. Res.*, **76,** 288–306.

Ziegler, C. L., and D. R. MacGorman, 1994: Observed lightning morphology relative to modeled space charge and electric field distributions in a tornadic storm. *J. Atmos. Sci.*, **51,** 833–851.

Zrnić, D. S., 1987: Three-body scattering produces precipitation signature of special diagnostic-value. *Radio Sci.*, **22,** 76–86.

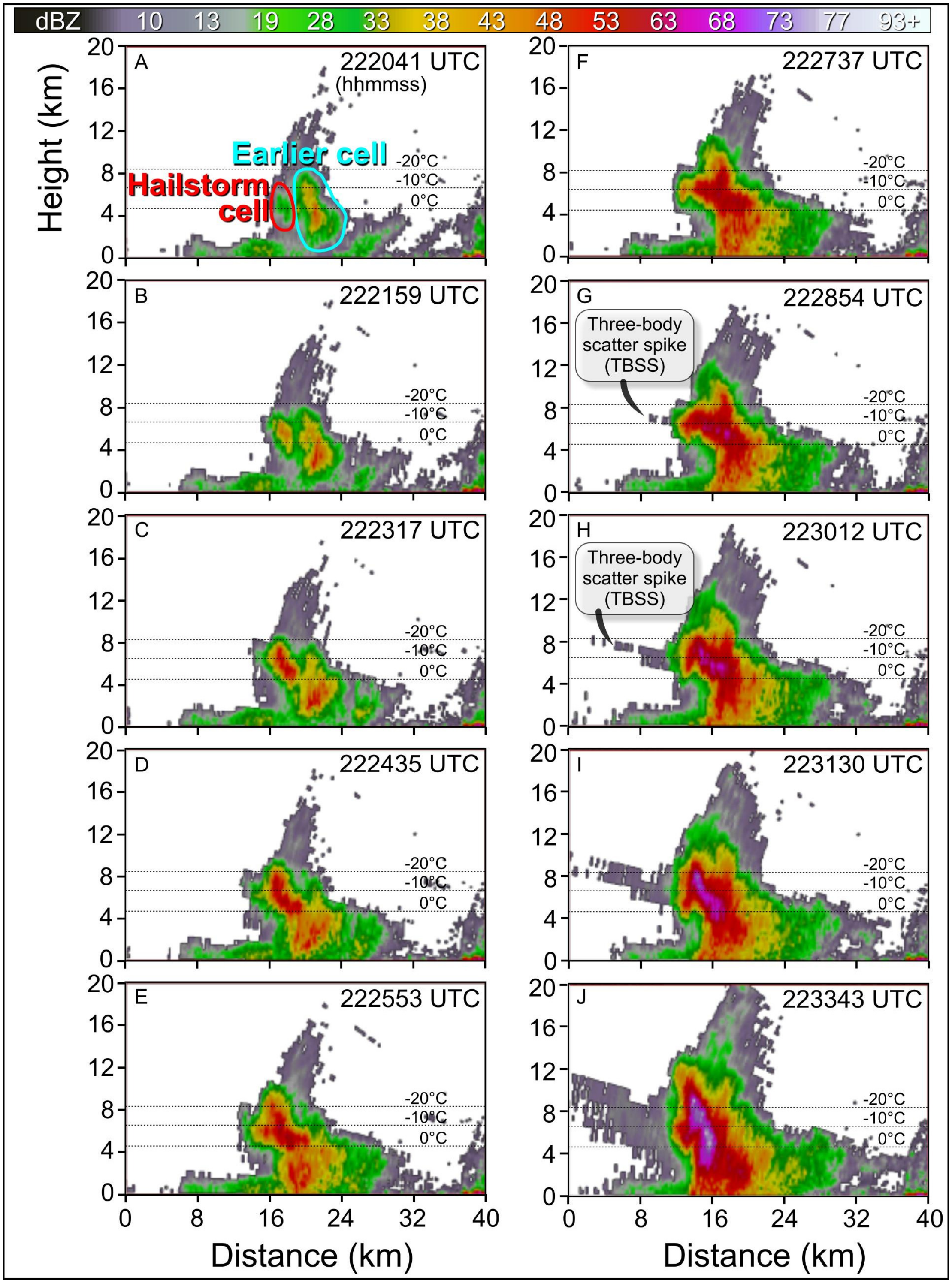

Fig. 1. First ~13 min of radar reflectivity data of the hail-producing storm on 15 Augist 2006 constituting period 1 of the storm (from Emerisic et al. 2011); to make the desired period fit on one page, 1-2 volume scans were skipped between each panel shown. Each panel shows a vertical cross section of reflectivity (dBZ) taken along a 40-km-long line along the azimuth through the storm's early reflectivity core. Increasing horizontal axis values correspond to decreasing distance from the NWRT PAR (0 is approximately 50 km from the NWRT PAR).

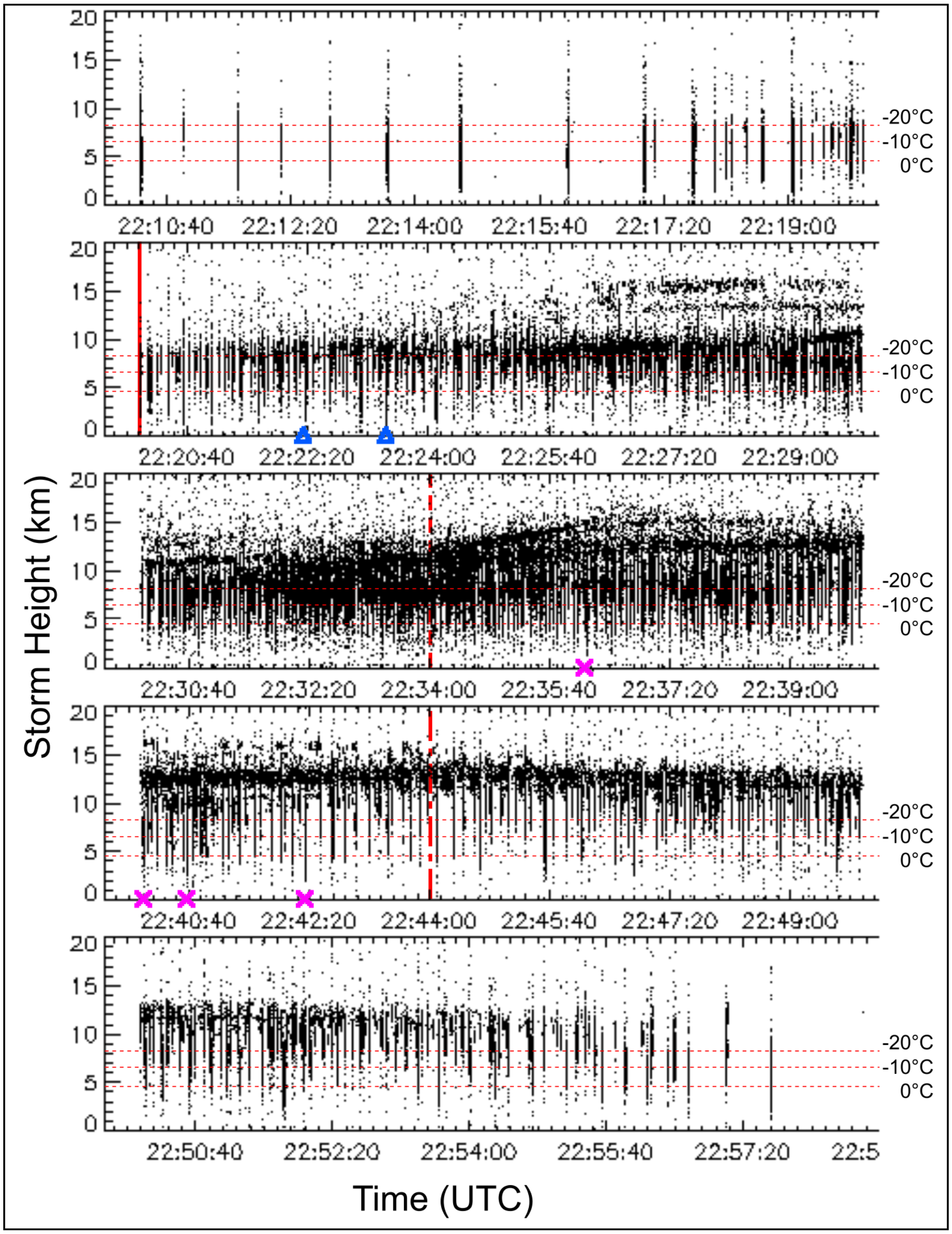

Fig. 2. The altitude and time of VHF sources mapped by the LMA (from Emersic et al. 2011). Individual black vertical line-like features denote individual flashes; during active periods, many such lines merge into general black regions. Symbols on the horizontal axis represent suspected ground lightning strike times of a given polarity detected by NLDN; blue triangles represent negative ground strikes; magenta crosses represent positive ground strikes. Solid red vertical line denotes start of period 1 of storm; dashed line represents start of period 2; dot-dash line represents start of period 3.

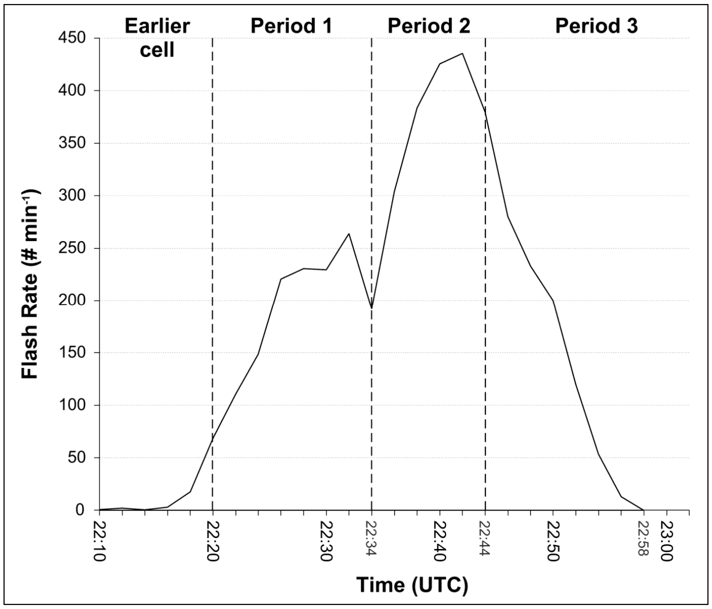

Fig. 3. Time-series plot of flash rates determined from OK-LMA data of the three storm lifecycle periods analyzed for this study (from Emersic et al. 2011).

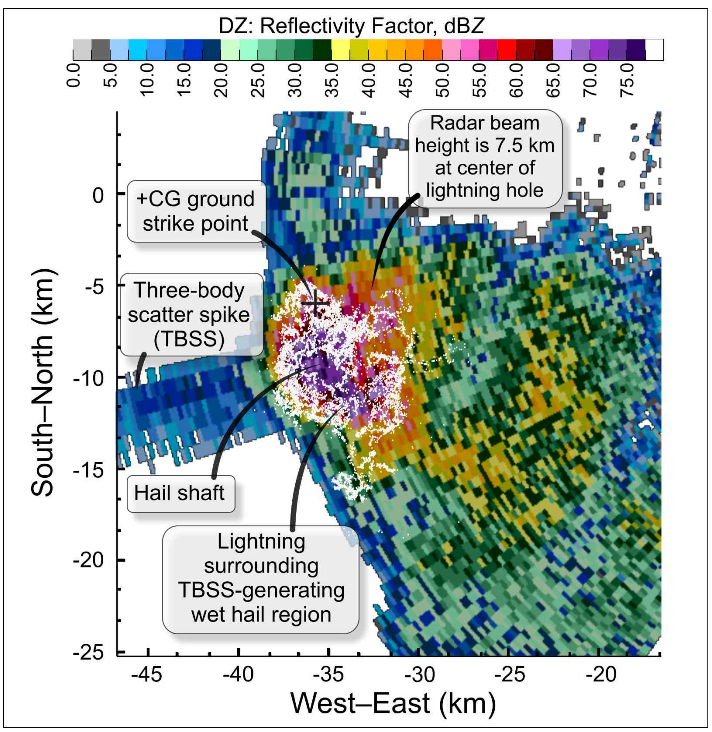

Fig. 4. Radar and LMA lightning data overlay of lightning surrounding the region in which hail is inferred from the TBSS to be in wet growth (from Emersic et al. 2011). Only lightning in the vicinity of the hail shaft is shown for clarity in viewing storm structure. The LMA data are from a 20-s period correlating closely with the time of the radar image. The distances shown are from the radar origin. The radar elevation here was 11°, corresponding to an altitude of 7.5 km at the center of the lightning hole.

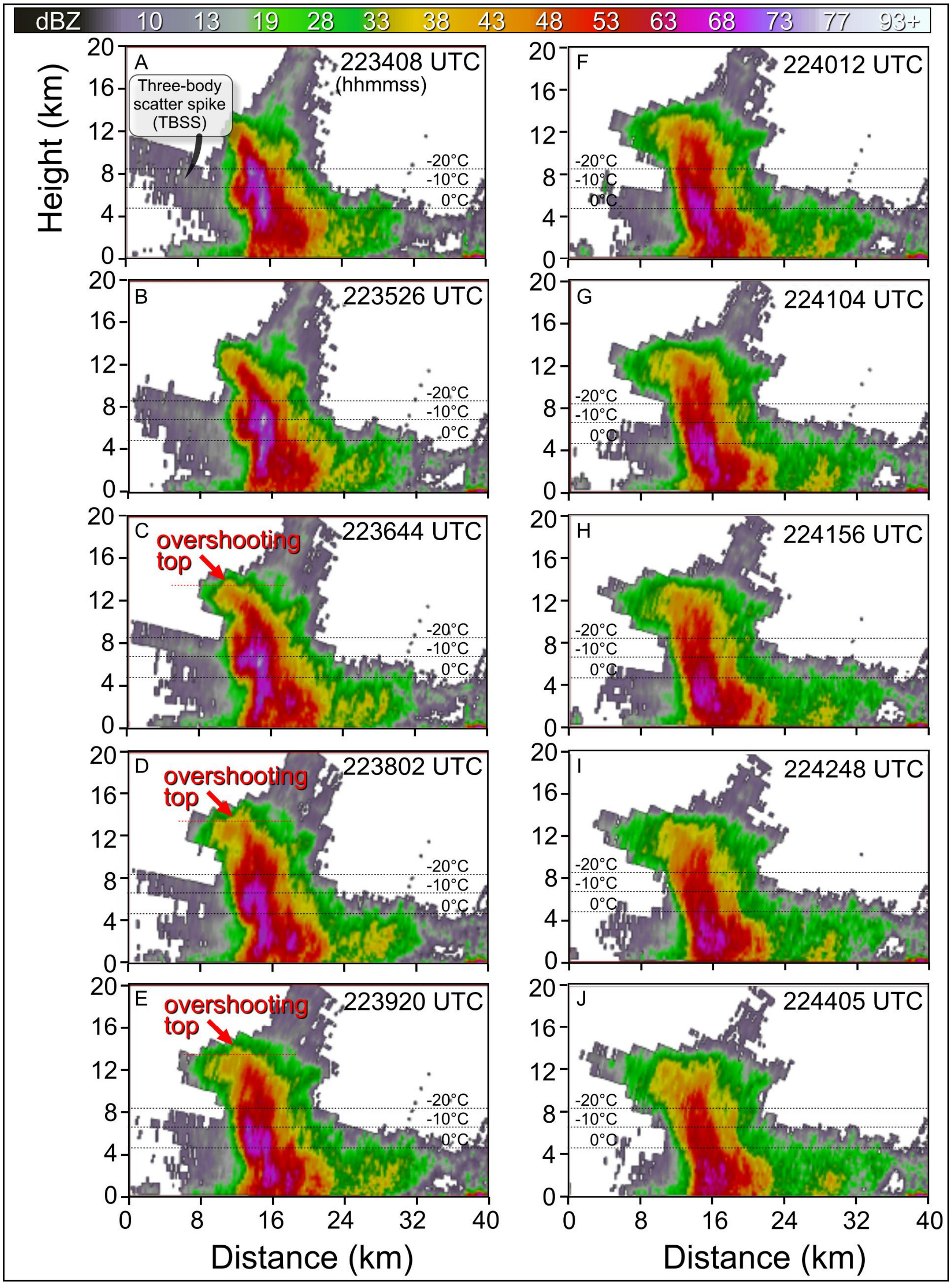

Fig. 5. Radar reflectivity for period 2 of the hail-producing storm on 15 August 2006 (from Emersic et al. 2011). See explanation in caption for Fig. 1.